Electronic spectroscopy of *trans*-azomethane by electron impact*

Oren A. Mosher†, Michael S. Foster†, Wayne M. Flicker, J. L. Beauchamp, and Aron Kuppermann‡

Arthur Amos Noyes Laboratory of Chemical Physics, § California Institute of Technology, Pasadena, California 91109
(Received 22 April 1974)

The electron impact excitation of *trans*-azomethane (i.e., *trans*-dimethyl diazine CH_3-N=N-CH_3) has been studied by both trapped electron (TE) and differential electron scattering (DES) techniques. The nature of the excited state in each of several transitions has been identified by the energy and angular dependences of the excitation cross section. Two previously unreported singlet–triplet transitions are observed with maxima at 2.75 and 4.8$_4$ eV. Theoretical calculations on the parent compound, *trans*-diimide (H-N=N-H), suggest that these are the $\tilde{X}\ ^1A_g \rightarrow 1\ ^3B_g$ (produced by excitation of an electron from an n_+ molecular orbital to a π^* molecular orbital) and the $\tilde{X}\ ^1A_g \rightarrow 1\ ^3B_u$ ($\pi \rightarrow \pi^*$) transitions, respectively. The $\tilde{X}\ ^1A_g \rightarrow 1\ ^1B_g$ ($n_+ \rightarrow \pi^*$) transition is observed with a peak at 3.50 eV in the DES studies. A strong peak at 6.01 eV in the TE spectra appears as a weak shoulder in the DES studies and is interpreted as either a symmetry-forbidden or Rydberg-like singlet–singlet transition. Allowed singlet–singlet features overlap each other in the transition energy range from 6 to 10 eV. Peaks are seen in the DES spectra at 6.71, 7.8, and 9.5 eV and in the TE spectrum at 8.0 eV. Several significant differences between the TE and the DES spectra are analyzed on the basis of the different nature of the two experiments.

I. INTRODUCTION

Azomethane is the simplest acyclic azoalkane. The photochemistry of azoalkanes has been reviewed by Collier *et al.*[1] and by Engel and Steel.[2] These molecules decompose following light absorption in the near ultraviolet to produce N_2 and two alkyl radicals[1,2] and thus are convenient sources of the latter species. The photochemical precursor state in each of several photochemical processes in the azoalkanes has not been clearly established. Elucidation of the nature of the precursor states has been hindered by a lack of any direct spectroscopic measurements of the energy of low-lying triplet excited states. In the present paper we describe studies employing both trapped electron (TE) and differential electron scattering (DES) techniques to locate these electronic states.

II. METHODS AND RESULTS

A. Sample preparation

Azomethane was prepared and handled as previously described.[3] Although the *cis*-isomer can be generated photolytically[4] under certain conditions, azomethane exists only in the *trans*-configuration[5] as commonly prepared, and we used this isomer throughout our studies. The mass spectrum was in good agreement with the published one.[6] The sample was subjected to several liquid nitrogen freeze–pump–thaw cycles prior to its use.

B. Trapped electron spectrum

The TE experiments were performed using an ion cyclotron resonance (ICR) spectrometer, as previously described.[7,8] In one set of experiments, using the CCl_4 scavenging method,[7] the threshold excitation spectrum was obtained by monitoring Cl^- ions produced by the dissociative attachment reaction of thermal energy electrons with CCl_4. In a second series of experiments employing the total negative current method,[8] no electron scavenger is used. In the present study of azomethane, the negative current consists solely of trapped electrons since no negative ions were detected when the incident electron energy was varied from 0 to 70 eV. Identical results were obtained with both the CCl_4 scavenging technique and the total negative current method.

Figure 1a shows the TE spectrum obtained by the total negative current method using a trapping voltage of -0.40 V in a conventional "flat" ICR cell. This corresponds to a well depth of 0.36 V.[9] Spectra run at smaller well depths were identical except for a generally poorer signal-to-noise ratio. The incident electron current was 1×10^{-7} A and the pressure of azomethane was 6×10^{-5} torr, as measured by a Schulz–Phelps ionization gauge. The energy scale was calibrated by identifying the $E\ ^3\Sigma_g^+$ peak of nitrogen at 11.87 eV[10] in its TE spectrum and assuming the energy scale correction to be independent of electron accelerating voltage.

C. Differential electron scattering spectra

The variable angle electron impact spectrometer is the one described previously[11] except that the inner and outer radii of the energy analyzers have been increased from 2.22 and 2.86 cm to 3.49 and 4.13 cm, respectively, and the lens support system has been modified to facilitate assembly and insure accurate alignment. A Spiraltron electron multiplier has replaced the previous discrete dynode multiplier.

Electron spectra were taken at impact energies of 20 eV, 40 eV, and 60 eV and scattering angles ranging from 10° to 80°. The gas in the scattering chamber was maintained at a pressure of about 4×10^{-3} torr as indicated by an uncalibrated Schulz–Phelps ionization gauge. The incident electron current was about 6×10^{-8} A. The instrumental resolution, defined as the full width at half maximum of the elastic peak, was chosen typically in the range 0.10 to 0.15 eV, except for a few spectra

run at 0.06 eV. Figures 1b, 2, and 3 show several DES spectra obtained under different conditions.[12]

Ratios of the differential cross section (DCS) of each spectral feature to that of the elastic peak or the singlet → singlet transition at 6.71 eV were determined from the areas under each peak as previously described.[13,14] The ratios to the 6.71 eV transition are displayed in Figs. 4 and 5.

The elastic DCS in arbitrary units shown in Figs. 6 and 7 were determined by multiplying the observed count rates by the scattering volume correction[15] appropriate for each scattering angle (θ) and normalizing the results to an arbitrary value of 1.0 at $\theta = 40°$. The reproducibility of these elastic DCS measurements is about 10%.

The DCS for the 6.71 eV transition between 20° and 80° was obtained by multiplying the DCS ratio of this transition with respect to the elastic peak by the elastic DCS at each θ. In addition, for angles of 30° and below, the DCS of this transition was obtained without reference to the elastic peak using the same procedure as for the elastic DCS, except that the normalization procedure

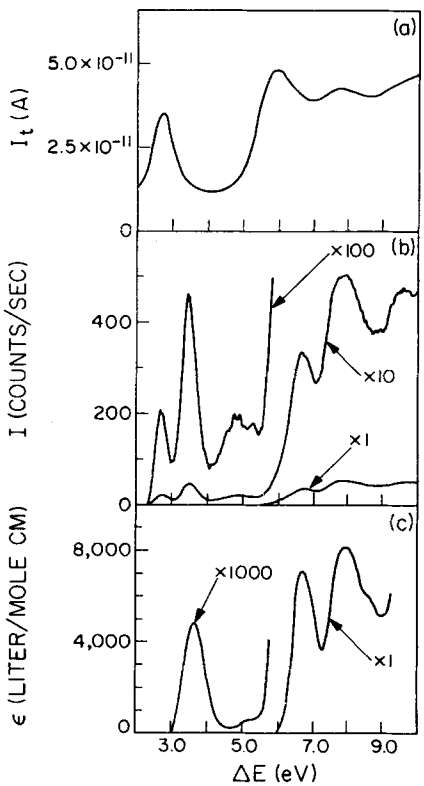

FIG. 1. (a) Trapped electron spectrum of azomethane. The ordinate I_t is the trapped electron current, for the following conditions: 1×10^{-7} A incident beam current; 6×10^{-5} torr sample pressure as read on an uncalibrated Schulz–Phelps gauge; 0.4 V well depth. (b) Electron energy-loss spectrum. The ordinate I is the scattered current at $\theta = 50°$; 40 eV incident electron energy; 7×10^{-8} A incident beam current; 3.6×10^{-3} torr uncalibrated Schulz–Phelps gauge sample pressure reading. (c) Optical absorption spectrum taken from figures in Refs. 1 and 17a. The ordinate ϵ is the molar extinction coefficient. For all curves the abscissa ΔE is the excitation energy.

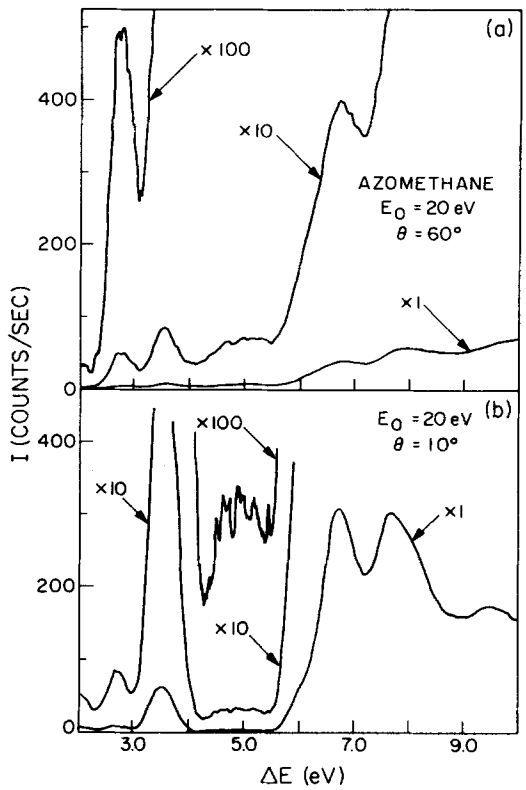

FIG. 2. Electron energy-loss spectrum of azomethane at (a) $\theta = 60°$ and (b) $\theta = 10°$; 20 eV incident electron energy; 1×10^{-8} A incident beam current; 4.4×10^{-3} torr uncalibrated sample pressure reading; 0.15 eV resolution (full width at half maximum of elastic peak).

was to make the result at 20° agree with that obtained by the ratio method. These two methods agreed well for the 6.71 eV transition DCS value at $\theta = 30°$.

The DCS curves for the other inelastic transitions displayed in Figs. 6 and 7 were determined by the ratio method using the elastic DCS as a reference for angles of 20° and above and the 6.71 eV transition DCS as a reference at $\theta = 10°$. The arbitrary units in Figs. 6 and 7 are the same for all curves displayed. Due to contributions of elastic DCS irreproducibility (~10%), inaccuracies in the ratio measurements associated with band overlaps, energy-loss dependent background count rates, and other instrumental effects, the overall accuracy in these relative inelastic DCS measurements is estimated to be 35% at scattering angles of 30° and above. At smaller angles, uncertainty in the volume correction can increase this inaccuracy.

III. DISCUSSION

A. The molecular orbital scheme in azomethane and diimide

Azomethane is known to exist in a *trans*-planar configuration in the gas phase and therefore possesses C_{2h} symmetry. The coordinate axes implied in the orbital designations used below are located as follows.

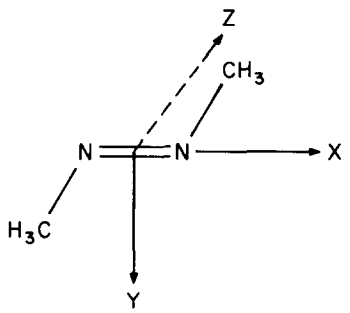

Only one calculation[16] of excited state energies has been performed on azomethane. This calculation used the zero-differential-overlap approximation and thus gave no estimate of the singlet–triplet splitting. Several studies[16–20] are available on the related molecule diimide. This molecule should provide a useful model for interpreting the lowest electronic states in azomethane provided that the appropriately localized orbitals involved in these states are relatively invariant[21,22] to replacement of the H atom by CH_3. Such chemically invariant orbitals correspond to the intuitive idea of chemical bonds in the molecule.

The presence of two N atoms in the diimide molecule leads to two "formally nonbonding" MO's, the symmetric (n_+) and antisymmetric (n_-) linear combinations of the lone pair orbitals on the two nitrogen atoms. The interaction between such nonbonding orbitals has recently been reviewed by Hoffmann.[23] Theoretical calculations for diimide[16–20] indicate that the highest filled orbital is the n_+ and that the energy splitting between it and n_- is large. The ground state has ^1A_g symmetry arising from a $1b_u^2 1a_g^2 2a_g^2 2b_u^2 3a_g^2 3b_u^2(n_-)\,1a_u^2(\pi)\,4a_g^2(n_+)$ configuration. The lowest excited states, the $1\,^3B_g$ and the $1\,^1B_g$, arise from an $n_+ \rightarrow \pi^*[\cdots 4a_g^2(n_+) \rightarrow \cdots 4a_g^1(n_+)\,1b_g^1(\pi^*)]$ excitation. The next state is the $1\,^3B_u(\pi \rightarrow \pi^*)$. The results of the theoretical studies of diimide are summarized in Table I.

The *ab initio* calculation of Robin *et al.*[17a] employed a Gaussian basis set to obtain a self-consistent field (SCF) ground state. The excited states were obtained by performing a limited configuration interaction (CI) calcula-

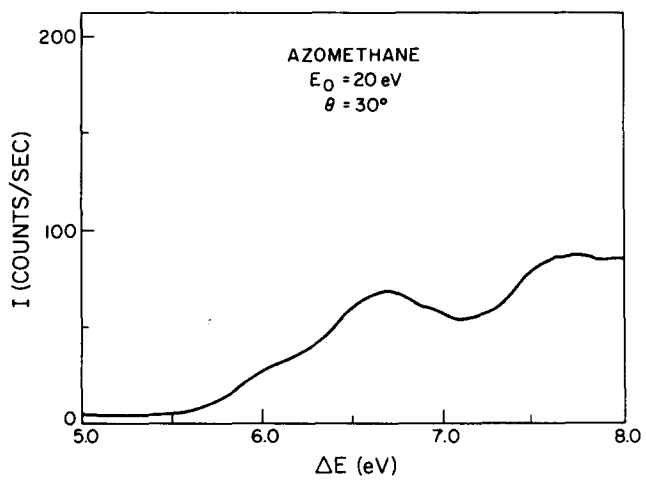

FIG. 3. Electron energy-loss spectrum of azomethane in the 5.0 to 8.0 eV energy-loss region for $\theta = 30°$; 20 eV incident electron energy; 3.5×10^{-3} torr uncalibrated sample pressure reading.

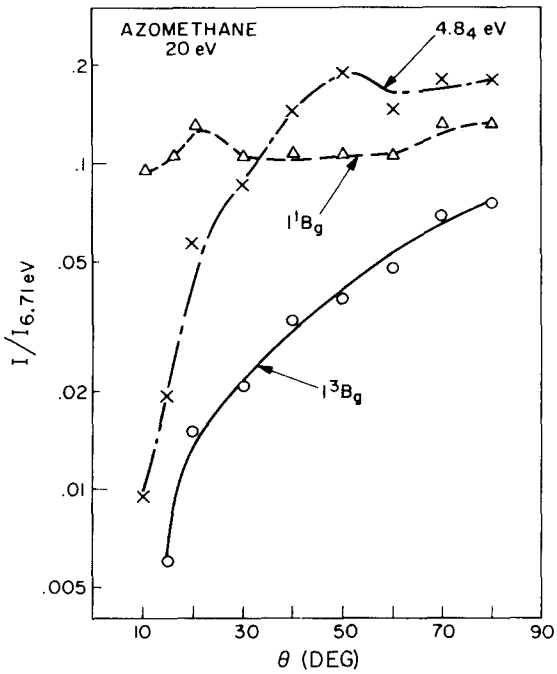

FIG. 4. Ratio of intensities I of several electronic transitions in azomethane to that of the 6.71 eV singlet → singlet transition ($I_{6.71\,eV}$) as a function of θ at an incident electron energy of 20 eV. The excited states for the curves shown are $1\,^3B_g$ (○), $1\,^1B_g$ (△), and the 4.84 eV (×).

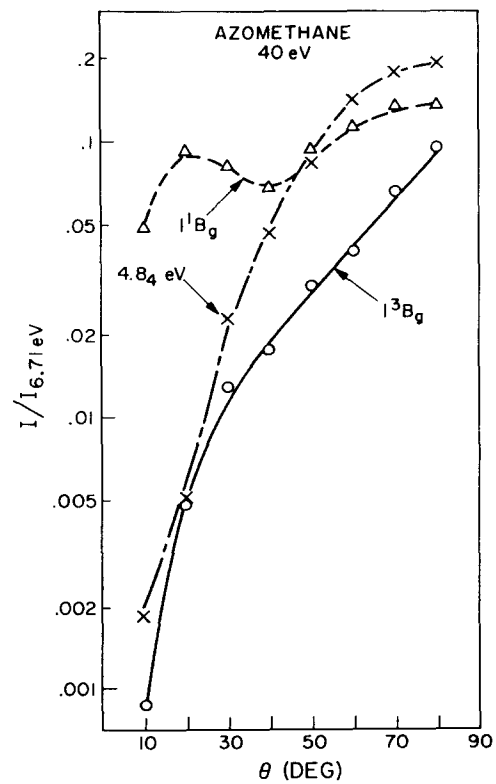

FIG. 5. Same as Fig. 4 at an incident electron energy of 40 eV.

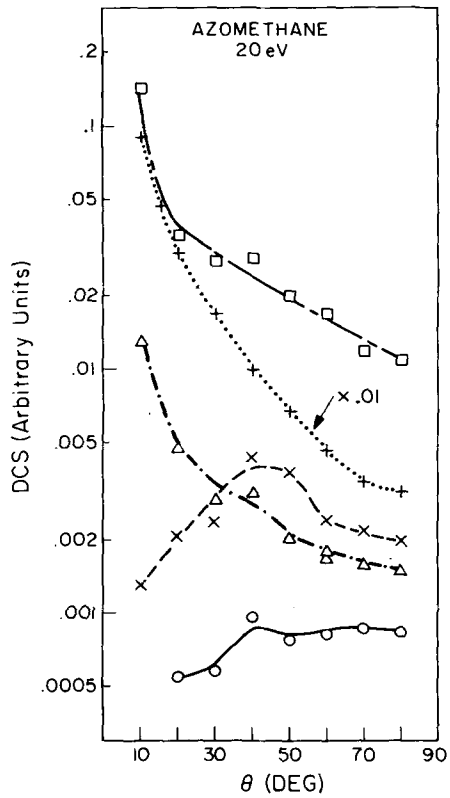

FIG. 6. Differential cross sections as a function of θ at an incident electron energy of 20 eV for elastic scattering (+) and for transitions to the following excited states: 1^3B_g(○), 1^1B_g(△), 4.8_4 eV triplet (×) and the 6.71 eV singlet (□).

tion involving configurations generated from the virtual orbitals of the ground state. Wagnière[16] also performed an *ab initio* calculation using a Gaussian basis set. The energies from his calculation listed in Table I are the differences between the open-shell SCF state energies and the lowest closed-shell SCF state energy. Wong, Fink, and Allen[18] calculated an *ab initio* SCF ground state using Gaussian lobe orbitals, and performed a separate calculation on the open shell 1^3B_g state. The orbitals in the 1^1B_g state were then assumed to be the same as in the 1^3B_g state.[24] Tinland[19] used the modified CNDO/2 method, a semiempirical approach, which involves an all-valence-electron CI. Winter and Pitzer[20] performed an SCF calculation in which they carried out extensive calculations on the ground state, using a Gaussian basis set. They obtained the excited state energies by optimizing only the open-shell orbitals, taking the remaining orbitals from the ground state calculations.

B. Trapped electron spectrum

As shown in Figure 1a, three prominent features appear in the TE spectrum of *trans*-azomethane with peaks at 2.72 ± 0.05 eV, 6.01 ± 0.05 eV and 8.0 ± 0.1 eV. The optical absorption spectrum[1,17a] has also been shown in Figure 1c for comparison. The lowest optically observed transition is the $\tilde{X}\,^1A_g \rightarrow 1\,^1B_g\,(n_+ \rightarrow \pi^*)$ peaking at 3.64 eV. Therefore, the state at 2.72 eV above the ground state is presumably the 1^3B_g. The possibility that this transition was due to a temporary negative ion resonance was eliminated by making measurements with well depths of 1.2 eV and noticing that the peak was still present. This assignment is further discussed in Sec. III. C. 1. The nature of the states corresponding to the higher energy peaks cannot be determined by the TE method alone because threshold electron impact can produce both spin-allowed and spin-forbidden excitations with comparable effectiveness.[25] The factors which determine relative peak intensities in TE spectra are further discussed in Sec. III.D.

C. Differential electron scattering spectra

Figure 1b shows the 2 to 10 eV energy-loss region at 40 eV impact energy and $\theta = 50°$, while Fig. 2 displays the 2 to 10 eV energy-loss region at 20 eV impact energy and scattering angles of 10° and 60°. Figure 3 shows the 5 to 8 eV energy-loss region at 20 eV incident electron energy and $\theta = 30°$. Peaks are seen at 2.75 ± 0.04, 3.50 ± 0.04, 4.8_4 ± 0.1, 6.71 ± 0.03, 7.8 ± 0.1, and 9.5 ± 0.1 eV in the DES spectra. Each feature is discussed in greater detail in the following sections, and the results are summarized in Table II.

1. The $1\,^3B_g$ $(n_+ \rightarrow \pi^*)$ state

A peak is observed with a maximum at 2.75 ± 0.04 eV and a Frank–Condon region from about 2.3 to 3.1 eV. The sharp increase with scattering angle of the ratio of the area under this peak to that of the strong singlet at

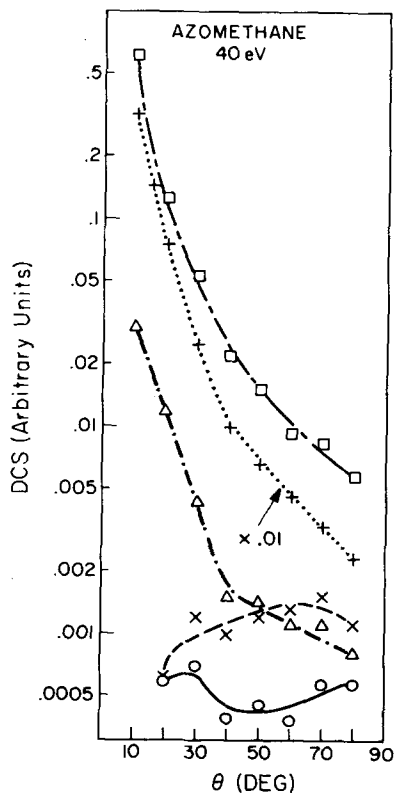

FIG. 7. Same as Fig. 6 for an incident electron energy of 40 eV.

TABLE I. Calculated electronic state energies of *trans*-diimide.

Orbitals involved in the transition	Upper state	Calculated transition energy (eV)				
		Wagniére[a]	Robin *et al.*[b]	Tinland[c]	Wong *et al.*[d]	Winter and Pitzer[e]
$n_+ \rightarrow \pi^*$	$1\,^3B_g$	1.75	3.01	2.60	3.22	1.8
$n_+ \rightarrow \pi^*$	$1\,^1B_g$	3.08	3.92	2.60	3.84	3.1
$\pi \rightarrow \pi^*$	$1\,^3B_u$	3.69	6.53	4.50		

[a]Reference 16.
[b]Reference 17a.
[c]Reference 19.
[d]Reference 18.
[e]Reference 20.

6.71 eV (see Sec. III.C.5), as shown in Figs. 4 and 5, is characteristic[11,13,14] of a spin-forbidden excitation. The magnitude and relative insensitivity to θ of the DCS for excitation of this state supports this conclusion. The position of this peak is in good agreement with the TE maximum occurring at 2.72 ± 0.05 eV.

Theoretical calculations[16–20] for diimide uniformly predict that the lowest triplet arises from an $n_+ \rightarrow \pi^*$ excitation and thus the 2.75 eV peak in azomethane most likely corresponds to the $\tilde{X}\,^1A_g \rightarrow 1\,^3B_g$ transition.

2. The $1\,^1B_g$ ($n_+ \rightarrow \pi^*$) state.

The second inelastic feature has a maximum at 3.50 ± 0.04 eV with an approximate onset and end of 2.9 and 4.2 eV, respectively. This transition, which in the optical spectrum has a maximum at 3.64 eV in the gas phase[1,17a] and at 3.47 eV in hydrocarbon solution,[26] has been assigned[17] to the $\tilde{X}\,^1A_g \rightarrow 1\,^1B_g$ ($n_+ \rightarrow \pi^*$) excitation. It is a spin-allowed but electric dipole-forbidden transition. The area ratio behavior shown in Figs. 4 and 5 and the forward peaking behavior of the DCS shown in Figs. 6 and 7 confirm the assignment to a spin-allowed transition. The absence of this transition in the TE spectrum is discussed in Sec. III.D.

3. The 4.8_4 eV triplet state

A broad, weak feature is observed with an apparent onset of 4.0 eV, a maximum at $4.8_4 \pm 0.1$ eV, and an end beyond 5.5 eV. The area ratio plots in Figs. 4 and 5 and the DCS curves in Figs. 6 and 7 are quite similar to the results obtained for the $\tilde{X}\,^1A_g \rightarrow 1\,^3B_g$ transition and confirm its singlet → triplet nature. This transition is not observed in the TE spectrum (see discussion in Sec. III.D.)

Theoretical calculations for diimide predict[16,17,19] that the second triplet state is the $1\,^3B_u(\pi \rightarrow \pi^*)$, but this assignment may not be applicable to azomethane because diimide may not properly describe the higher energy states in azomethane.

The optical absorption spectrum (see Fig 1c) in this region[1] shows a horizontal inflection point at about 5.1 eV with an extinction coefficient of about 0.5 liter/mole cm. A rough estimate of the oscillator strength f for this region using a classical dispersion theory formula[27] gives $f = 4 \times 10^{-6}$, which is relatively large but still within the estimated range[28] of f values for $\pi \rightarrow \pi^*$ singlet → triplet excitations. However, this optical feature need not correspond to the 4.8_4 eV triplet; it could instead[29] be due to a 0.01% impurity having an extinction coefficient of $\epsilon = 5 \times 10^3$ liter/mole · cm. Such an ϵ is typical of many optically allowed transitions.

4. The 6.01 eV singlet state

The TE spectrum shows a strong peak at 6.01 eV, while many of the DES spectra show a weak shoulder around 6.0 eV energy loss. Figure 3 shows this feature in more detail. The slope break is noticeable in both low and high angle spectra. This suggests that it is due to a weak singlet → singlet transition which may either be symmetry forbidden or of a Rydberg type. The strong intensity in the TE spectrum also establishes that it is not due to a singlet → singlet transition of an impurity in the sample. A discussion of the relative strength of this

TABLE II. Excited electronic states of *trans*-azomethane.

Excited state	Nature of transition	Transition energy (eV)		
		TE	DES	Optical[a]
$1\,^3B_g$	$n_+ \rightarrow \pi^*$	2.72 ± 0.05	2.75 ± 0.04	...
$1\,^1B_g$	$n_+ \rightarrow \pi^*$	...	3.50 ± 0.04	3.64
Triplet ($1\,^3B_u$?)	$\pi \rightarrow \pi^*$ if ^3B_u	...	$4.8_4 \pm 0.1$	5.1?
Singlet	Symmetry forbidden or Rydberg-like	6.01 ± 0.05	$6.0_1 \pm 0.1$	...
Singlet	Optically allowed		6.71 ± 0.03	6.75
		8.0 ± 0.1	7.8 ± 0.1	7.95
			9.5 ± 0.1	

transition in the TE and DES spectra is given in Sec. III.D.

Robin *et al.*[17a] have attributed a weak feature (extinction coefficient of about 1 to 5 l/mole · cm)[30] peaking at 5.48 eV in their optical spectrum to the symmetry-forbidden $\tilde{X}\,^1A_g \rightarrow 2\,^1A_g$ transition. The DES spectra show an onset around 5.4 eV but do not have any observable peak at 5.5 eV energy loss. Thus the 6.0 eV feature appears to be unrelated to the state at 5.48 eV. Robin has since suggested[30] that the 5.48 eV optical peak may reflect the presence of a small amount of photochemically produced[4] *cis*-azomethane in the sample or that it may be due to a very minor impurity.

5. *Higher singlet states*

The first strong feature in the DES spectrum has a maximum at 6.71 ± 0.03 eV. The DCS curves shown in Figs. 6 and 7 are characteristic of optically allowed singlet → singlet transitions.[11] This is confirmed by the fact that such a transition appears in the optical spectrum at about 6.75 eV.[17a] Additional strong singlet → singlet transitions are seen at 7.8 ± 0.1 and 9.5 ± 0.1 eV. Our DES spectra as well as the optical one[17a] give some indication that an additional singlet state may exist in the neighborhood of 8.5 eV. The TE spectrum shows a peak at 8.0 eV superimposed on a background from the strongly overlapped singlet or triplet states in this energy region.

D. Comparison of differential electron scattering and trapped electron spectra

A comparison of the DES and TE spectra shows that several significant differences exist between these two types of electron impact spectra. The reason for these differences is that the spectra reflect different electron impact properties. In the DES spectra, the ordinate is proportional to the magnitude of the differential scattering cross section, at the impact energy and scattering angle being considered, corresponding to the energy loss given by the abscissa. In the TE spectra the ordinate is proportional to the derivative of the total cross section with respect to impact energy, in the neighborhood of the excitation energy threshold represented by the abscissa.[25,31]

As mentioned in Sec. III.C.2, the $\tilde{X}\,^1A_g \rightarrow 1\,^1B_g$ transition is not observed in the TE spectrum shown in Fig. 1a. The absence of this transition in the TE spectrum indicates that, at threshold, its excitation cross section rises quite slowly compared to those of the observed singlet → triplet and singlet → singlet transitions. A variety of TE studies have shown that singlet → singlet transitions may be absent or very weak in the TE spectrum. The $1\,^1S \rightarrow 2\,^1P$ transition in He is very strong in the DES spectrum[11] but shows up only as a small shoulder on the high energy side of the $1\,^1S \rightarrow 2\,^3P$ peak in the TE spectrum[25,31] As another example, the $\tilde{X}\,^1\Sigma^+ \rightarrow {}^1\Pi$ transition in CO appears very weakly in the TE spectrum[31] but is a strong feature in the DES spectra.[11]

In Sec. III.C.3 it was noted that the 4.8_4 eV triplet feature appeared in the DES spectrum but not in the TE one. This suggests that its cross section increases slowly with increasing energy in the threshold region. Analogous behavior occurs in 1, 3-butadiene, where the $\tilde{X}\,^1A_g \rightarrow 1\,^3A_g$ transition is easily seen by the DES method[13,14] but is very weak in the TE spectrum.[32]

Sec. III.C.5 contains an example of an inverse behavior, in which the transition at 6.0 eV occurs strongly in the TE spectrum but very weakly in the DES spectrum. Further differences between the two methods are also seen in the energy-loss region from 6 to 10 eV as shown in Figures 1a and 1b.

Therefore, the absence of a transition from a TE spectrum and its presence in a DES or optical spectrum does not imply a disagreement between the different techniques. Furthermore the presence in the TE spectrum of an intense feature does not necessarily correlate with its optical absorption coefficient or DES strength. As a result, great caution should be exercised in interpreting TE spectra without comparing them with other kinds of electronic spectra.

IV. CONCLUSIONS

The results of the TE and DES spectral studies presented in this paper and an analysis of earlier work lead to several conclusions. The lowest excited electronic state is the $1\,^3B_g(n_+ \rightarrow \pi^*)$ peaking at 2.72 eV in the TE study and 2.75 eV in the DES spectra. A second triplet state is observed at 4.8_4 eV. The analogy with diimide suggests that this is the $1\,^3B_u(\pi \rightarrow \pi^*)$ state. The lowest excited singlet state, the $1\,^1B_g(n_+ \rightarrow \pi^*)$ at 3.50 eV in the DES spectrum, is excited by an electric dipole-forbidden transition from the ground state. A prominent peak is seen at 6.01 eV in the TE spectrum, while it occurs as a weak shoulder in the DES spectra. The weakness of this transition in both the DES and optical spectra suggests that it is either a symmetry-forbidden or a Rydberg-type singlet → singlet transition with an excitation cross section which increases sharply with electron energy near threshold. Additional strongly allowed singlet → singlet transitions produce overlapped bands in the 6 to 10 eV transition energy region. The results of this study illustrate the importance of interpreting TE spectra in conjunction with other types of electronic spectra.

ACKNOWLEDGMENTS

We thank Dr. M. B. Robin, Dr. N. W. Winter, and Dr. W. A. Goddard III for several helpful discussions. We also thank Dr. Winter for communication of his theoretical results prior to their publication.

*Work supported in part by the United States Atomic Energy Commission under Grant Numbers AT(04-3)-767 PA No. 4 and AT(04-3)-767-8 awarded to A. Kuppermann and J. L. Beauchamp, respectively. Report Code CALT-767P4-131.

†Work performed in partial fulfillment of the requirements for the Ph.D. degree in Chemistry at the California Institute of Technology.

‡To whom correspondence on this paper should be addressed.

§Contribution No. 4870.

[1]S. S. Collier, D. H. Slater, and J. G. Calvert, Photochem. Photobiol. 7, 737 (1968).
[2]P. S. Engel and C. Steel, Acc. Chem. Res. 6, 275 (1973).
[3]M. S. Foster and J. L. Beauchamp, J. Am. Chem. Soc. 94, 2425 (1972).
[4]R. F. Hutton and C. Steel, J. Am. Chem. Soc. 86, 745 (1964).
[5]C. H. Chang, R. F. Porter, and S. H. Bauer, J. Am. Chem. Soc. 92, 5313 (1970).
[6]Z. Prâsil and W. Forst, J. Am. Chem. Soc. 90, 3344 (1968).
[7]D. P. Ridge and J. L. Beauchamp, J. Chem. Phys. 51, 470 (1969).
[8]T. McAllister, Chem. Phys. Lett. 13, 602 (1972).
[9]T. B. McMahon and J. L. Beauchamp, Rev. Sci. Instrum. 42, 1632 (1971).
[10]G. Herzberg, *Molecular Spectra and Molecular Structure* I (Van Nostrand, Princeton, 1950), p. 551.
[11]S. Trajmar, J. K. Rice, and A. Kuppermann, Adv. Chem. Phys. 18, 15 (1970).
[12]Count rates in spectra taken at different angles and impact energies can be compared only after changes in incident electron current, scattering volume, and sample gas pressure are taken into account.
[13]O. A. Mosher, W. M. Flicker, and A. Kuppermann, Chem. Phys. Lett. 19, 332 (1973).
[14]O. A. Mosher, W. M. Flicker, and A. Kuppermann, J. Chem. Phys. 59, 6502 (1973).
[15]S. Trajmar, D. C. Cartwright, J. K. Rice, R. T. Brinkmann, and A. Kuppermann, J. Chem. Phys. 49, 5464 (1968).
[16]G. Wagniére, Theor. Chim. Acta 31, 269 (1973).
[17](a) M. B. Robin, R. R. Hart, and N. A. Kuebler, J. Am. Chem. Soc. 89, 1564 (1967); (b) M. B. Robin and W. T. Simpson, J. Chem. Phys. 36, 580 (1962).
[18]D. P. Wong, W. H. Fink, and L. C. Allen, J. Chem. Phys. 52, 6291 (1970).
[19]B. Tinland, Spectrosc. Lett. 3, 51 (1970).
[20]N. W. Winter and R. M. Pitzer (private communication).
[21]S. F. Boys, Rev. Mod. Phys. 32, 296 (1960).
[22]W. England, L. S. Salmon, and K. Ruedenberg, Fortschr. Chem. Forsch. 23, 31 (1971).
[23]R. Hoffmann, Acc. Chem. Res. 4, 1 (1971).
[24]As Wong *et al.*[18] note in their paper, the approximations involved in this open-shell calculation make the results somewhat suspect.
[25]G. J. Schulz, Phys. Rev. 112, 150 (1958).
[26]G. Kortuem and H. Rau, Ber. Bunsenges. Phys. Chem. 68, 973 (1964).
[27]W. Kauzmann, *Quantum Chemistry* (Academic, New York, 1957), p. 581.
[28]S. P. McGlynn, T. Azumi, and M. Kinoshita, *Molecular Spectroscopy of the Triplet State* (Prentice-Hall, New Jersey, 1969), p. 20.
[29]C. Steel reports in a private communication that the bump at 5.1 eV disappears when the azoalkane is rigorously purified.
[30]M. B. Robin (private communication).
[31]H. Brongersma, A. J. H. H. Boerboom, and J. Kistemaker, Physica 44, 449 (1969).
[32]H. H. Brongersma, Ph. D. thesis, University of Leiden, Leiden, The Netherlands, 1969.